Yu et al. Virology Journal (2025) 22:65
https://doi.org/10.1186/s12985-025-02680-3

Virology Journal

RESEARCH

Open Access

Identification of a novel small-molecule inhibitor of the HIV-1 reverse transcriptase activity with a non-nucleoside mode of action

Kyung-Lee Yu[1], YoungHyun Shin[1], Dong-Eun Kim[1], Jeong-Ah Kim[2], Jeong-Eun Kang[1], Pooja Singh[3], Keun Woo Lee[4,5], Chul Min Park[6], Hojin Kwon[7], Sunwoo Kim[7], Songmee Bae[1] and Cheol-Hee Yoon[1*]

Abstract

Background Human immunodeficiency virus-1 (HIV-1) is the causative agent of acquired immunodeficiency syndrome, which is a major global health problem. Although combination antiretroviral therapy (cART) successfully expands the lifespan of HIV-1-infected patients, long-term cART often increases drug resistance and adverse effects. Therefore, efforts are ongoing to develop novel anti-HIV-1 drugs.

Methods The anti-HIV-1 activities of compounds were investigated using TZM-bl reporter cell line, A3.01 T cell line, and peripheral blood mononuclear cells infected with several HIV-1 strains, including wild type and drug-resistance associated mutants. Next-generation sequencing analysis and in silico molecular docking studies were employed to determine the mode of action of the compound.

Results We identified a small-molecule inhibitor consisting of a thiadiazole core appended to two pyrazoles (BPPT), which exerted a highly potent inhibitory effect on HIV-1 infectivity, with a half-maximal effective concentration (EC_{50}) of 60 nM, without causing cytotoxicity. In experiments with various HIV-1 strains and cell types, the potency of BPPT was found to be comparable to that of commercial antiretroviral agents (azidothymidine, nevirapine, and others). Further analysis of the mode of action demonstrated that BPPT is a novel type of HIV-1 non-nucleoside reverse transcriptase inhibitor (NNRTI). Analysis of viruses harboring drug-resistance-associated mutations showed that BPPT was potent against G190A (C or S) mutations in reverse transcriptase (RTase), exhibiting high-level resistance to other NNRTIs. Next-generation sequencing analysis of long-term treatment with BPPT displayed an RTase mutation profile different from that in the case of established NNRTIs. Given these data, in silico molecular docking studies demonstrated the molecular mechanism underlying the BPPT-mediated inhibition of RTase.

Conclusion Our data suggest that BPPT is a novel small-molecule inhibitor of HIV-1 RTase and could serve as a promising chemical scaffold to complement or replace conventional treatments, particularly for overcoming resistance associated with the G190 mutation.

Keywords Thiadiazole derivative, Anti-HIV-1 activity, Reverse transcription, Drug-resistance mutation

*Correspondence:
Cheol-Hee Yoon
kmc755@korea.kr
Full list of author information is available at the end of the article

Introduction

Acquired immune deficiency syndrome, caused by human immunodeficiency virus-1 (HIV-1) infection, is one of the most challenging health problems worldwide [1]. Although combination antiretroviral therapy (cART) successfully represses the viral load, it often leads to drug resistance-associated mutations, adverse side effects, and poor patient compliance with long-term administration [2]. Additionally, latently HIV-1-infected reservoirs cells established during early infection persist in patients and are not eradicated even with cART [3–5]. Therefore, exploring new anti-HIV-1 drug candidates with higher potency, novel targets, and fewer side effects is an ongoing research interest [6].

Several strategies for suppressing the HIV-1 life cycle have been investigated; these include interruption of the CCR5 attachment of viral gp120 [7, 8], fusion of virus-host membranes [9], reverse transcription (RT) [10, 11], and integration and virion maturation [12, 13]. RT, accomplished by viral reverse transcriptase (RTase), has been a key target for developing agents against HIV-1 infection for a long time since HIV-1 was identified, and RTase inhibitors (RTIs) are the main components in cART regimens [14]. RTIs are classified into two categories based on their binding to the catalytic and hydrophobic allosteric sites of RTase. Nucleoside RTase inhibitors (NRTIs) are structural analogs lacking the 3′-hydroxyl group of nucleoside(tide) (Fig. 1A) and are converted to their phosphorylated active form by cellular kinases [15]. Phosphorylated NRTIs bind to the catalytic site of the p66 subunit of RTase and are subsequently incorporated into viral cDNA during RT, followed by the termination of viral DNA synthesis [10, 16]. Non-nucleoside reverse transcriptase inhibitors (NNRTIs) bind to a hydrophobic pocket near the catalytic site of the p66 subunit of RTase (Fig. 1A), leading to structural changes within the active site of RTase and interference with viral DNA polymerization [17–19]. The advantages of the NNRTI-class of RTase inhibitors, including no cellular phosphorylation compared with the some NRTIs, have prompted the identification of more than 60 diverse chemical scaffolds as NNRTIs [20]. The United States (U.S.) Food and Drug Administration (FDA) has approved six clinical drugs (nevirapine (NVP), delavirdine (DLV), efavirenz (EFV), etravirine (ETR), rilpivirine (RPV), and doravirine (DOR)), and the Russian Ministry of Health has approved elsulfavirine (VM-1500A or ESV) [21]. The binding mode of these drugs involves interactions with residues L100, K101, K103, V106, V179, Y181, Y188, G190, F227, W229, and M230 in the hydrophobic pocket of RTase [22, 23]. However, high-level resistance-associated mutations, such as L100I, K101E/P/Q, K103N, Y181C, Y188L, E138K, and G190A/S, impose restrictions on the clinical use of these inhibitors [24].

Diverse screening approaches, such as structure-based drug design and computational virtual and biochemical/biophysical screening, are currently available for anti-HIV-1 drugs. Functional screening assays based on reporter cells are widely used in initial screening approaches because of their advantages in displaying antiviral activity relevant to physiological conditions.

In this study, we employed a TZM-bl reporter cell line assay, which is widely used as a validated standard platform for HIV-1 vaccine and drug development [25, 26], to identify novel agents against the early phase of HIV-1 infection from a compound library. The assay results were verified with orthogonal assays including diverse HIV-1 strains and cellular systems. We identified a chemical scaffold containing a thiadiazole core appended to two pyrazoles (hereafter, referred to as BPPT). The compound selectively inhibited the RTase activity with a mode of action similar to that of NNTRIs, resulting in the inhibition of viral replication. In addition, the mechanism

(See figure on next page.)

Fig. 1 Anti-viral activity of BPPT in various cell types. **A** Chemical structures of BPPT and currently approved reverse transcriptase (RTase) inhibitors and illustration of etravirine bound to the hydrophobic pocket of RTase. The illustration of the crystal structure has been adapted from previously deposited data [72]. **B** TZM-bl cells (1×10^4) infected with HIV-1_{NL4-3} at a multiplicity of infection (MOI) of 0.5 were treated with two-fold (left panel) and five-fold (right panel) serial dilutions of BPPT. After 48 h of infection, the firefly luciferase (F-Luc) activity, indicating viral infectivity (red line), and cell viability (black line) were determined using the Bright-Glo luciferase assay kit and PrestoBlue Cell Viability Reagent, respectively. **C** TZM-bl cells (5×10^4) cultured in 24-well plates were infected with HIV-1_{NL4-3}IRES-eGFP virus along with the indicated compounds. After 48 h of treatment, GFP-expressing cells were observed using fluorescence microscopy (×200 magnification) and the count of GFP-positive cells was determined using flow cytometry. The concentrations of the compounds were as follows: BPPT (0.01, 0.1, 1, and 10 μM); zidovudine (AZT, 5 μM); efavirenz (EFV, 1 μM); dolutegravir (DTG, 1 μM). **D** A3.01 cells (5×10^4) infected with HIV-1_{NL4-3} at an MOI of 0.1 were treated with five-fold serial dilutions of BPPT for 3 days. The p24 levels (red line) in the cell supernatant were determined using the HIV-1 p24 ALPHALISA kit. The cell viability (black line) was determined as described above. **E** Peripheral blood mononuclear cells (PBMCs; 4×10^5) infected with HIV-1_{NL4-3} (purple line) or HIV-1_{JRCSF} (pink line) at an MOI of 0.1 were treated with five-fold serial dilutions of BPPT. The levels of p24 were determined using the HIV-1 p24 ALPHALISA kit after 3 (HIV-1_{JRCSF}) or 4 (HIV-1_{NL4-3}) days. In parallel, the cell viability (black line) was determined at 4 days, as described above. **B**, **D**, **E** The dose–response curves show the relative activity compared with that of the dimethyl sulfoxide (DMSO) control (mean ± SD; $n = 3$)

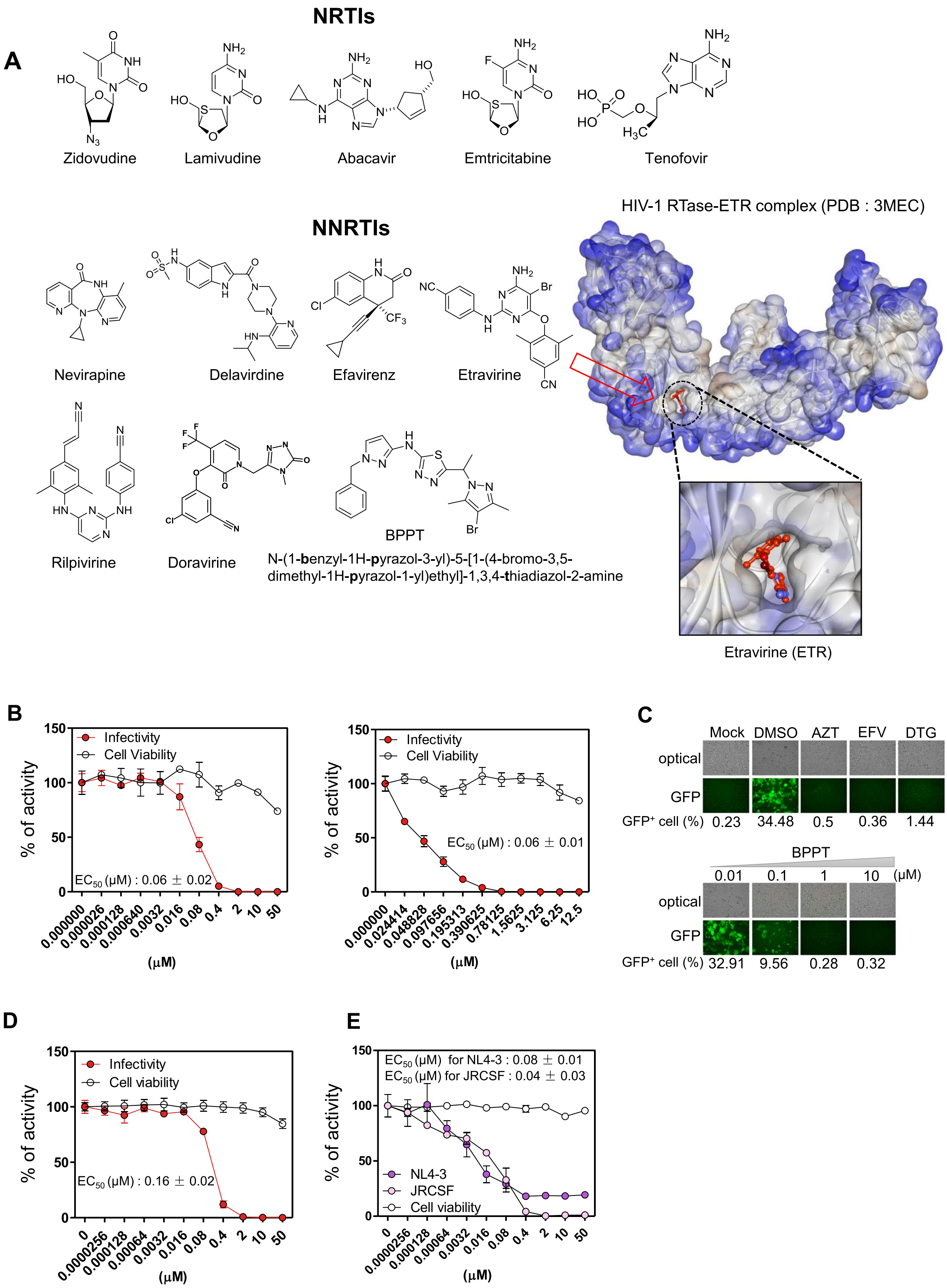

Fig. 1 (See legend on previous page.)

of action of BPPT was elucidated using in vitro resistance selection and in silico docking studies.

Materials and methods

Cell lines and reagents

TZM-bl cells (also referred to as JC53BL-13) [27] expressing human CD4, CXCR4, and CCR5 and the human T cell line A3.01 were provided by the National Institute of Health (NIH) HIV Reagent Program (Bethesda, MD, USA). HEK293T (CRL-3216) cell line was purchased from the American Type Culture Collection (ATCC, Manassas, VA, USA). TZM-bl and HEK293T cells were cultured in Dulbecco's modified Eagle's medium (DMEM) supplemented with 1% penicillin–streptomycin sulfate (Gibco-BRL, Waltham, MA, USA) and 10% fetal bovine serum (FBS) (Hyclone, Logan, UT, USA). A3.01 cells and peripheral blood mononuclear cells (PBMCs) (AllCells, Alameda, CA, USA) were cultured in RPMI medium (Invitrogen, Waltham, MA, USA) or RPMI medium supplemented with IL2 and pytohemagglutinin M (PHA-M) for PBMCs, as previously described [28].

A compound library was obtained from the Korea Chemical Bank (KCB) (www.chembank.org) of the Korea Research Institute of Chemical Technology (KRICT). The library consists of 16,771 compounds selected randomly from ~ 375,000 compounds deposited in KCB, which were collected from various sources, including pharmaceutical companies and research institutions. All compounds were dissolved in dimethyl sulfoxide (DMSO) at 5 mM and stored in 96-well plates at − 20 °C. Plates were sealed with coated aluminum foil to prevent evaporation and cross-contamination. BPPT was initially provided by the KCB of the KRICT, and custom synthesized by ChemDiv (San Diego, CA, USA). The purity of synthetic BPPT was confirmed to be greater than 95% with ^{1}H-NMR spectra data provided by the manufacturer and our LC/MS and high-resolution mass spectrometry (HRMS) data (Fig. S2). Enfuvirtide (T-20), zidovudine (AZT), EFV, NVP, and triptolide (TPL, an HIV-1 transcriptional inhibitor) were purchased from Sigma Aldrich (St. Louis, MO, USA). Dolutegravir (DTG), raltegravir (RAL), RPV, lopinavir (LPV), and ritonavir (RTV) were purchased from Sellek Chem (Houston, TX, USA). All the compounds were synthesized at purity exceeding 90% or 95%, as evaluated using high-performance liquid chromatography.

Viruses

The HIV-1 molecular clones, including pNL4-3, p89.6, ARV-resistant HIV-1 strains (ARP-7396, ARP-7406, ARP-7407, ARP-12227, ARP-12231, ARP-12241, and ARP-12243) [29, 30], and HIV-1 encoding green fluorescent protein (GFP) (ARP-11349: HIV-1_{NL4-3}-IRES-eGFP) [31] were provided by the NIH HIV Reagent Program. Each molecular HIV-1 clone was transfected into HEK293T cells, as described previously [32] to obtain infectious HIV-1 particles. Virus-containing cell culture supernatants were collected two days after transfection and filtered through a 0.45 μm membrane filter (Millipore Sigma, Burlington, MA, USA) to remove cell debris, aliquoted, and frozen at − 80 °C for future infections. Viral titration was performed as described previously [33]. In brief, 1×10^4 of TZM-bl cells seeded in 96-well plates were infected with 200 μL of virus-containing medium diluted two-fold serially, in triplicate. Two days later, infectious viral particles were titrated using the beta-Galactosidase staining kit (Mirus Bio, Madison, WI, USA). The titer of infectious virus preparation was determined as the mean value of the blue-colored cell count × dilution factor and was used to determine the multiplicity of infection (MOI) in each infection experiment.

To construct clones with mutations in the RT region, site-directed mutagenesis was performed using the overlap extension PCR method [34]. Briefly, PCR products for the overlapping template were prepared using site-directed mutagenesis with two separate PCR amplifications. The PCR amplifications were performed with ApaI forward and mutagenic reverse primer pairs, and mutagenic forward and AgeI reverse primer pairs, respectively, using the pNL4-3 template. The overlap PCR was performed with ApaI forward and AgeI reverse primer sets using the first two mutated PCR products as templates. The PCR product was then inserted into the ApaI/AgeI site of pNL4-3 using the respective restriction enzymes. The PCR amplification was performed using the PrimeSTAR® max DNA polymerase (Takara, Japan). The primer sequences are listed in supplementary Table 1.

Antiviral activity

The inhibitory effects of the compounds on HIV-1 infection were determined as previously described [32]. Briefly, 1×10^4 TZM-bl cells were seeded in white 96-well cell culture plates. After 24 h, the compounds were added at the indicated concentrations, and the virus infection was done at an MOI of 0.5. After 48 h of infection, the inhibitory effect on viral infection was determined by measuring the firefly luciferase (F-Luc) activity using BioTek Synergy H1 (Agilent Technologies, Santa Clara, CA, USA) with the Bright Glo™ luciferase assay kit (Promega). GFP-expressing cells infected with HIV-1_{NL4-3}-IRES-eGFP were visualized using fluorescence microscopy (IX83, Olympus, Japan) and counted using flow cytometry (FACSLyric, Becton Dickinson, Franklin Lakes, NJ, USA).

A3.01 cells (5×10^4) or PBMCs (4×10^5; pre-activated with PHA-M for 3 d) were infected with HIV-1 strains at an MOI of 0.1 with spinoculation at $300\times g$ for 2 h at 25 °C. After infection, the cells were washed with fresh medium and cultured with the indicated concentrations of the compounds. PBMCs were supplemented with 10 international units (IU)/mL of IL-2. After 72 or 96 h of infection, the inhibitory effect on viral replication was determined by measuring the amount of viral capsid protein (p24) in the cell culture medium using an HIV-1 p24 ALPHALISA kit (PerkinElmer, Waltham, MA, USA).

Cell viability test

To assess the cytotoxicity of the compounds, cells were prepared and treated with the compounds in parallel with assays for anti-HIV-1 activity, as described above, except for viral infection to avoid the cytopathic effects of the virus. Cell viability was determined using the PrestoBlue Cell Viability Reagent (Thermo Fisher Scientific, Waltham, MA, USA), following the manufacturer's instructions.

Time-of-addition (TOA) assay

The TOA assay was performed as described previously [35]. Briefly, 1×10^4 TZM-bl cells were infected with HIV-1 at an MOI of 0.5 and subsequently treated with the compounds at the indicated time points. At 48 h postinfection, viral infectivity was determined by measuring the F-Luc activity with BioTek Synergy H1 (Agilent Technologies) using a Bright Glo™ luciferase assay kit.

HIV-1 reverse transcription assay

The in vitro RTase assay was performed using the EnzChek™ Reverse Transcriptase Assay Kit (Invitrogen) and recombinant HIV-1 RTase protein (Abcam, Cambridge, MA, USA) as previously described [36, 37]. Briefly, the poly(A) ribonucleotide template and oligo $d(T)_{16}$ primer were annealed for 1 h at room temperature (24 °C). Subsequently, the template/primer solution was diluted (1:200 in polymerization buffer), and 20 µL/reaction was aliquoted into a 96-well black/clear bottom microplate. Recombinant HIV-1 RTase (0.5 unit) was added with or without the indicated concentrations of compounds and incubated for 1 h at 24 °C. The reaction was then stopped by adding 200 mM EDTA. The RNA–DNA heteroduplexes elongated by the RTase activity were incubated with the PicoGreen reagent capable of incorporation into the RNA–DNA duplexes for 5 min, and then detected with BioTek Synergy H1, using excitation and emission wavelengths of 480 and 520 nm, respectively.

The amount of HIV-1 reverse transcripts in cells infected with HIV-1 was measured using quantitative real-time PCR (RT-qPCR), as described previously [38, 39]. The HIV-1_{NL4-3} stock solution was treated with 100 units of DNase I (Roche) for 30 min at 37 °C to remove the transfected plasmid DNA. A3.01 cells (1×10^6) were infected with DNase I-treated infectious or heat-inactivated (for 30 min at 70 °C) virus at an MOI of 0.5 with spinoculation at $300\times g$ for 2 h at 24 °C. After infection, the cells were treated with 1 µM of the indicated compounds for 6 h in a 6-well cell culture plate. Total cellular DNA was extracted using the G-Spin™ DNA extraction kit (Intron Bio Tech, Seongnam-si, Gyeonggi-do, Republic of Korea), following the manufacturer's instructions. The amounts of early and late reverse transcripts were quantified using a 7500 Real-Time PCR System (Applied Biosystems) with each primer pair, as described previously [38, 39]. The amount of PCR products was normalized against β-globin. The primer and probe sequences are listed in Supplementary Table 1.

HIV-1 integration assay

The HIV-1 integrase activity was determined using an HIV-1 integrase assay kit (Xpress Bio, Frederick, MD, USA), as described previously [32]. In brief, a 96-well plate coated with donor substrate (DS) DNA was blocked with prewarmed blocking buffer for 30 min at 37 °C. One hundred µL of diluted HIV-1 integrase (1:300 in reaction buffer) was added to the plate and incubated for 30 min at 37 °C. After three washing steps, 50 µL of the indicated compounds was added to the plate at a final concentration of 10 µM and incubated for 5 min at 24 °C. Subsequently, 50 µL of diluted target substrate (TS) DNA (1:100 in reaction buffer) was added to the plate and incubated for 30 min at 37 °C. The plate was washed and then incubated with horseradish peroxidase (HRP)-conjugated antibody for 30 min at 37 °C. The integrase activity was estimated by determining the peroxidase activity with 3,3′,5,5′-tetramethylbenzidine (TMB) peroxidase substrate by measuring the absorbance at 450 nm. Detection of the integrated proviral DNA was performed using *Alu*-LTR-based real-time nested PCR (*Alu*-PCR), as described previously [40], with minor modifications. In brief, 1×10^6 A3.01 cells were infected with HIV-1 as described for the quantification of HIV-1 reverse transcripts. After infection, the cells were treated with 1 µM of the indicated compounds for 24 h. Thereafter, total cellular DNA was extracted. The 1st PCR was conducted as follows: 1 µL each of forward and reverse *Alu* primers (10 µM), 0.5 µL of ULF1 primer (10 µM), 12.5 µL of PrimeSTAR® max DNA polymerase (Takara, Japan), 5 µL sample DNA (100 ng), and 1 µL of H_2O were mixed in a final volume of 25 µL. The mixture was preheated to 94 °C for 2 min and then subjected to 15 cycles of 94 °C for 30 s, 55 °C for 30 s, and 72 °C for 3 min. The samples were then held at 72 °C for 5 min. The 2nd round of RT-qPCR was performed as follows: 1 µL each of forward and reverse primers (10 µM), 2 µL of probe primer (10 µM), 5 µL of tenfold diluted 1st round PCR product, 2 µL of H_2O, and 10 µL of probe qPCR mix with UNG (TaKaRa) were mixed, preheated to 95 °C for 2 min, and then subjected to 40 cycles of 95 °C for 15 s and 60 °C for 1 min. The amount of integrated proviral product was quantified using a 7500 Real-Time PCR System (Applied Biosystems). The PCR products were normalized against CD3. The primer and probe sequences are listed in Supplementary Table 1.

Drug combination assay

The combinatorial antiviral activity was determined based on the EC_{50} values of the compounds (drugs) against HIV-1 infectivity. The EC_{50} values of each drug were determined in this and other studies [41–43], and the virus inhibition rate was compared between compounds alone and in combination with BPPT (1:1 ratio of EC_{50}). The antiviral activities of BPPT combined with NRTIs (EFV and AZT) and integrase strand transfer inhibitors (INsTIs; RAL and DTG) were determined in TZM-bl cells. TZM-bl cells (1×10^4) were seeded in white 96-well cell culture plates. After 24 h, the cells were infected with HIV-$1_{NL4\text{-}3}$ at an MOI of 0.5 and treated with the indicated compounds at their EC_{50} for 2 days. The combinatorial assays of BPPT with protease inhibitors (PRIs; LPV and RTV) were conducted in A3.01 cells. A3.01 cells (5×10^4) infected with HIV-$1_{NL4\text{-}3}$-IRES-eGFP at an MOI of 0.2 were treated with the indicated compounds. After 4 days of infection, the inhibitory effect on viral replication was analyzed using flow cytometry (FACSLyric). The cell viability was determined using the PrestoBlue Cell Viability Reagent (Thermo Fisher Scientific) under the same conditions as used for the compounds without viral infection.

In vitro selection of antiviral resistance mutations

A3.01 cells (1×10^5) were infected at an MOI of 0.5 and simultaneously treated with 60 nM of BPPT, 1 nM of EFV, or 0.7 nM of RPV according to their EC_{50} values. Twenty percent of infected cells were passaged every 3–4 days with twofold increase in drug concentration whenever the p24 level in the collected viral supernatant exceeded 20% of that in the no-drug control. Viral RNA was extracted from viral supernatants using a QIAmp viral RNA kit (Qiagen) on days 36, 39, and 52. The viral RNA was converted into cDNA using RT-PCR with SuperScript™ III reverse transcriptase (Invitrogen), and the RT region (nt 2441–3959 of pNL4-3) was then PCR-amplified using PrimeSTAR® max DNA polymerase (Takara). The quality and quantity of the amplified PCR products were assessed using a NanoDrop 8000 spectrophotometer (Thermo Fisher Scientific) and a Qubit 3.0 Fluorometer (Invitrogen). Libraries were prepared using an Illumina DNA Prep Kit (Illumina, San Diego, CA, USA), according to the manufacturer's instructions. Libraries were purified and normalized to a concentration of 4 nM before pooling. The pooled library was denatured using 0.2 N sodium acetate and diluted to a final concentration of 9.2 pM. The library was spiked with 20% PhiX Control V3 (Illumina). Amplicon sequencing was performed on a MiSeq platform (Illumina) using a MiSeq Reagent Nano Kit V2 (300-cycles) (Illumina). FASTQ files were trimmed to eliminate low-quality reads and adapter sequences, assembled, extracted, and aligned with reference sequences (pNL4-3) using the default settings in the CLC Genomics Workbench software version 24 (Qiagen, Germantown, MD, USA). For excluding minor variation noise, the cutoff value was chosen as 0.5% based on a no-drug control error rate > 0.4%.

Molecular docking studies

Molecular docking is an established protocol in the field of computational biology for the identification of binding poses and molecular interaction patterns of receptor–ligand complexes [44–46]. The Cdocker module embedded in Discovery Studio (DS) was used to perform the molecular docking study [47–49]. The crystal structure of HIV-1 RTase bound to the FDA-approved drug EFV was downloaded from the Protein Data Bank (PDB: 1IKW) [50]. Prior to molecular docking studies, all heteroatoms and water molecules that did not participate in protein–ligand interactions were removed, and hydrogen atoms were added. The Clean Protein module, available in DS, was used for protein preparation [47]. All missing atoms were added and the bond orders were corrected. The prepared protein was then minimized using the CHARMm27 force field [51]. The NNRTI-binding pocket of the RTase was specified within the 10 Å radius of the bound drug, EFV. The 3D structures of chemical compounds were also prepared and energy minimized using the minimization tool in DS. A maximum of ten poses was generated for each molecule subjected to molecular docking using the GOLD Genetic Algorithm. EFV, bound to the crystal structure of HIV-1 RTase, was used as a reference for docking analysis.

Statistical analysis

All statistical analyses were performed using Prism (v.5.0; GraphPad, San Diego, CA, USA). All data are expressed as the mean ± SD ($n = 3$) and were compared using one-way ANOVA and Dunnett's multiple comparison test, with $^{*}p < 0.05$, $^{**}p < 0.01$, and $^{***}p < 0.001$ considered to indicate significant differences.

Results

Identification of a compound that inhibits HIV-1 infection in early stages

To discover inhibitory compounds capable of inhibiting HIV-1 infection in the early stages, initial screening assays using TZM-bl cells ($CD4^+$, $CXCR4^+$, and $CCR5^+$) harboring HIV-1 long terminal repeat (LTR) promoter-driven firefly luciferase, which is activated by the Tat protein expressed early after HIV-1 infection, were carried out with a library of 16,771 compounds at a final concentration of 6.25 μM. One hundred seventy-one compounds exhibited over 50% inhibition of viral infectivity at this concentration. The 2nd round of confirmatory test revealed five compounds exhibiting varying degrees of dose-dependent inhibitory effects on viral infection, showing over 50% cell viability at 12.5 μM (Fig. S1). The screened compounds were as follows: compound 1: 4-(2-oxo-2H-pyran-5-carboxamido)naphthalene-1-sulfonic acid (half maximal effective concentration (EC_{50}) = 8.48 μM); compound 2: 4-ethyl-7-((1-oxo-1-phenylbutan-2-yl)oxy)-2H-chromen-2-one (EC_{50} = 4.89 μM); compound 3: 3-tert-butyl-2-hydroxy-5-nitrobenzaldehyde (EC_{50} = 1.47 μM); compound 4: 1-amino-3-[(2,3-dimethoxyphenyl)methylideneamino]thiourea (EC_{50} = 6.39 μM); and compound 5: N-(1-benzyl-1H-pyrazol-3-yl)-5-[1-(4-bromo-3, 5-dimethyl-1H-pyrazol-1-yl) ethyl]-1,3,4-thiadiazol-2-amine (EC_{50} = 0.06 μM) (Fig. S1). Of these, compound 5, N-(1-benzyl-1H-pyrazol-3-yl)-5-[1-(4-bromo-3, 5-dimethyl-1H-pyrazol-1-yl) ethyl]-1,3,4-thiadiazol-2-amine (BPPT), exhibited the most potent antiviral activity with no cytotoxicity. The BPPT structure consists of a thiodiazole core symmetrically appended with anrylpyrazole and bromopyrazole. (Fig. 1A). To evaluate the antiviral activity of BPPT, a dose–response test using serial dilutions of BPPT was performed in TZM-bl cells. BPPT exhibited an EC_{50} of 0.06 μM against CXCR4 tropic HIV-1_{NL4-3} infection in experiments with twofold (ranging from 0.024414 to 12.5 μM) and fivefold (ranging from 0.000026 to 50 μM) serial dilutions and no severe cytotoxicity up to 250 μM (Figs. 1B and S3A, B). In the TZM-bl cell assay, BPPT also exhibited considerable inhibitory effects on the CCR5-tropic HIV-1_{JRCSF} and CXCR4/CCR5-dual tropic HIV-$1_{89.6}$ strains with EC_{50} values of 0.16 and 0.09 μM, respectively (Fig. S4 and Table 1). To further evaluate the potency of BPPT using other reporter systems, the cells were infected with HIV-1 encoding GFP (HIV-1_{NL4-3}-IRES-GFP) after treatment with BPPT. As shown in Fig. 1C, similar to the other ARVs (AZT, EFV, and DTG), BPPT inhibited the GFP signaling in a dose-dependent manner.

To determine the inhibitory effect of BPPT on whole viral replication, A3.01 T cells infected with NL4-3 (Fig. 1D) and PBMCs infected with NL4-3 or JRCSF HIV-1 strains (Fig. 1E) were treated with a serial dilution set of BPPT. BPPT efficiently inhibited the viral replication cycle in these cells with EC_{50} values of 0.16 μM and 0.08 or 0.04 μM, respectively, without causing any cytotoxicity up to 50 μM. The potency of BPPT was similar to that of NVP but less than that of EFV under our experimental conditions (Fig. 1D, E, and Table 1).

Determination of the mode of action of BPPT

To determine the mode of action of BPPT, a TOA assay was performed with well-defined ARVs inhibiting distinct steps in HIV-1 infection, including the entry inhibitor (T-20), NRTIs (AZT, NNRTI EFV), INsTIs (DTG and RAL), and viral transcription inhibitor (TPL). The inhibitory effect of BPPT disappeared when it was administered at 6 h postinfection, which was later than

Table 1 Antiviral activity of BPPT

Compounds	Virus	Cells	Assay	EC_{50}[a] (1:5 dilution) (μmol/L)	CC_{50}[b] (1:5 dilution) (μmol/L)	SI[c]
BPPT	NL4-3 (X4)	TZM-bl	Luc	0.06 ± 0.01	> 50	> 833
		A3.01	p24	0.16 ± 0.02	> 50	> 313
	JRCSF (R5)	TZM-bl	Luc	0.16 ± 0.01	> 50	> 313
	89.6 (X4/R5)	TZM-bl	Luc	0.09 ± 0.00	> 50	> 556
	NL4-3 (X4)	PBMCs	p24	0.08 ± 0.01	> 50	> 625
	JRCSF (R5)	PBMCs	p24	0.04 ± 0.03	> 50	> 1,250
EFV	NL4-3 (X4)	TZM-bl	Luc	0.001 ± 0.00	25.87	25,870
NVP				0.08 ± 0.18	> 50	> 625

[a] The half maximal effective concentration

[b] The half of the cytotoxic concentration

[C] The selective index were calculated by ration of EC_{50}/CC_{50}

that in the case of T20 (1 h) and AZT (2 h), but faster than that for DTG (8 h), RAL (8 h), and TPL (24 h). The time-dependent inhibition curve of BPPT was similar to that of EFV (Fig. 2A). To determine whether BPPT exerts an inhibitory effect on virus production, HEK293T cells were transfected with HIV-1_{NL4-3}-IRES-GFP proviral DNA and treated with BPPT for 48 h. The GFP signal expressed in transfected cells (Fig. 2B) and the level of p24 in the supernatant from transfected cells (Fig. 2C) were not inhibited by BPPT treatment. These data indicate that BPPT does not affect the late stages after intact viral DNA synthesis, including viral transcription, assembly, and release of viral particles. In contrast, BPPT treatment did not inhibit the Tat-mediated viral transcription of LTR in bl-DTR cells that simultaneously expressed Tat-mediated LTR-driven F-Luc and Renilla luciferase (R-Luc) upon doxycycline treatment (Fig. S5). F-Luc indicates the Tat-mediated viral transcriptional activity and R-Luc indicates the cellular transcriptional activity as an expression control (47). The results shown in Fig. 2A–C indicate the possibility that BPPT is an NNRTI. To clarify this, in vitro assays of RTase and integrase were performed in the presence of BPPT. BPPT directly inhibited the RTase activity in a dose-dependent manner (Fig. 2D), but did not affect the integrase activity even at a high dose (10 μM) (Fig. 2E). The half-maximal inhibitory concentration (IC_{50}) of BPPT against RTase was 0.14 μM, which was higher than that of EFV (0.012 μM) but lower than that of NVP (46.41 μM) (Fig. 2D). To determine whether BPPT inhibits the RT activity in cells infected with HIV-1, A3.01 cells were infected with HIV-1_{NL4-3} under BPPT treatment; 6 h later the levels of early and late RT products were determined using RT-qPCR (Fig. 2F), and 12 h later, the levels

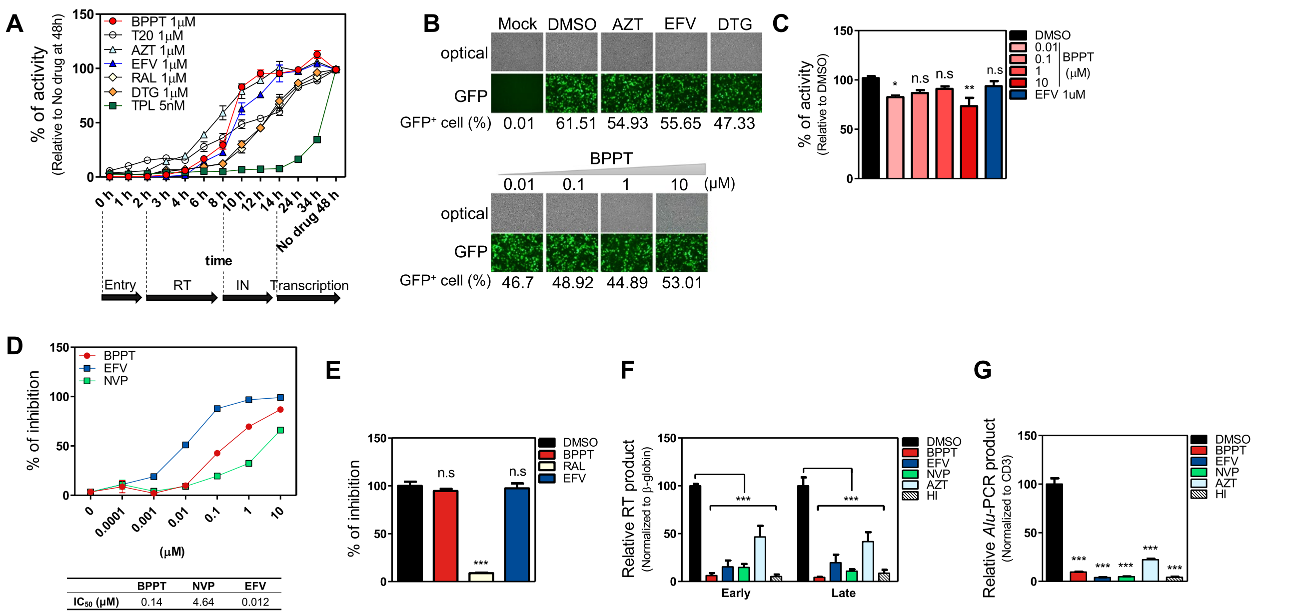

Fig. 2 Determination of the mode of action of BPPT. **A** Time-of-addition assay. TZM-bl cells (1×10^4) were infected with HIV-1_{NL4-3} at an MOI of 0.5. Subsequently, the cells were treated with the compounds at the indicated time points. At 48 h postinfection, the viral activity was measured as the F-Luc activity using the Bright-Glo luciferase assay kit. The relative activities are expressed as the mean ± SD ($n=3$) compared with that in the DMSO control measured after 48 h of infection. The time frames associated with each HIV-1 infection step are represented based on susceptibility to the well-known drugs. RT: reverse transcription, IN: integration. **B** and **C**. HEK293T cells (1.5×10^5) were transfected with 200 ng of the pBR43IeG-nef⁺ plasmid. Subsequently, the cells were treated as described for Fig. 1C. After 48 h, the GFP-expressing cells were observed using fluorescence microscopy (×200 magnification) (**B**), the count of GFP-positive cells was determined using flow cytometry (**B**), and the amount of viral production was measured using the p24 ALPHALISA™ kit (**C**). ****p* < 0.001, ***p* < 0.01, and **p* < 0.05, compared with the cells treated with DMSO. n.s.: non-significant. **D** An in vitro HIV-1 RT assay was performed with BPPT, EFV, and NVP, as described in "Materials and Methods." **E** An in vitro HIV-1 integrase assay was performed with BPPT (10 μM), EFV (10 μM), and raltegravir (RAL, 10 μM), as described in "Materials and Methods." Data are expressed as the mean ± SD ($n=3$) compared with the DMSO control. **F** A3.01 cells (1×10^6) infected with DNase I-treated active or heat-inactivated HIV-1_{NL4-3} at an MOI of 1 were treated with the indicated compounds (1 μM). After 6 h of infection, viral reverse transcription (RT) product (viral cDNA) was extracted; its level was determined using quantitative real-time PCR (RT-qPCR) and represented as the mean ± SD ($n=3$) normalized against β-globin compared with that in cells treated with DMSO. **G** A3.01 cells (1×10^6) infected with DNase I-treated HIV-1_{NL4-3} at an MOI of 1 were treated with the indicated compounds (1 μM). After 24 h of infection, the level of integrated viral DNA was determined using *Alu*-PCR, as described in "Materials and Methods." The relative activity is expressed as the mean ± SD ($n=3$) compared with the DMSO control. **C** and **E**–**G** ****p* < 0.001, compared with the DMSO control. n.s.: non-significant

of chromosome-integrated viral DNA were determined using *Alu*-based qPCR (Fig. 2G). BPPT greatly inhibited the synthesis of viral cDNA in both the early and late stages of RT, and the inhibitory effect at the RT stage resulted in the detection of a low level of integrated proviral DNA, similar to that observed for other (N)NRTIs. These results indicate that BPPT is a potent inhibitor of RTase, comparable to the currently used NNRTIs.

Antiviral effect of BPPT on (N)NRTI-resistant HIV-1 variants

To evaluate the antiviral activity of BPPT against (N)NRTI-resistant variants, BPPT or ARVs were used to treat cells infected with recombinant viruses containing NRTI- and NNRTI-resistant mutations, and their susceptibilities were determined (Table 2 and Fig. S6A). The recombinant 7396 virus containing only NRTI-resistance mutations was fully susceptible to BPPT and EFV, and four-fold less susceptible to NVP than the wild-type virus. In contrast, the susceptibility to NNRTIs and BPPT was markedly reduced in strains containing NNRTI resistance-associated mutations. The 7406 virus containing a G190C mutation was highly resistant to NVP and EFV, but was slightly resistant to BPPT. BPPT and EFV exhibited similar levels of resistance to the 7407 strain harboring K103N, represented as 328.17- and 350 fold-changes (FCs) in EC_{50} compared with that for the wild-type virus, respectively. The strains containing multiple NNRTI resistance-associated mutations, 12,227 (K101P/K103N), 12,231 (K103N/V179F/Y181C), and 12,243 (K100I/V179D/M230L), exhibited high resistance to either BPPT or the established NNRTIs. However, the 12,241 (K101E/138G/G190S) virus was more susceptible to BPPT than to NNRTIs. These results support the possibility that the G190C(S) substitution on RT may be much less resistant to BPPT than to other NNRTIs.

To further explore the effect of NNRTI resistance-associated single mutations on susceptibility to BPPT, recombinant HIV-1 variants containing a single mutation associated with NNRTI resistance were constructed. TZM-bl cells were infected with an equivalent MOI of each recombinant for 48 h following treatment with BPPT or ARVs. The EC_{50} values and FCs in EC_{50} compared with those for the wild-type virus are listed in Table 3 and their dose–response inhibitory curves are shown (Fig. S6B). Substitutions at positions 181 (Y181C, Y181V) or 188 (Y188L) significantly abolished the activity of BPPT, NVP, and EFV. The L100I substitution conferred a higher degree of resistance to BPPT (FC = 58.33) than to NVP (FC = 2.20) or EFV (FC = 15). The K101P and K103N substitutions induced moderate resistance to BPPT, with FCs of 28.50 and 13.75, respectively. V106M substitution, known to be resistant to several NNRTIs, showed no resistance to BPPT, whereas, the mutation induced moderate resistance to current NNRTIs, including DOR, except RPV (Table 3 and Fig. S7). Although BPPT exhibited no resistance to the V106M substitution, the antiviral activity of BPPT was less than that of DOR and RPV (Fig. S7). Notably, the substitutions (G190A, G190C, and G190S) at position 190 exhibited the highest resistance to NVP (FCs = 195.75–408.63) and EFV (FCs = 12–390), whereas these mutations were susceptible to BPPT (FCs = 1.09–4.588). The susceptibility of BPPT to the G1901C substitution was similar to that of the 7406 strain containing the G190C substitution. Indeed, the G190A mutation did not confer resistance to BPPT. AZT showed no resistance to NNRTI

Table 2 Antiviral effect of BPPT on clinically derived multi-drug resistant variants

Virus[a]	Major NNRTI RAMs	Major NRTI RAMs	EC_{50} (μM)[b] (Fold change, FC)[c]			
			BPPT	EFV	NVP	AZT
WT			0.06 ± 0.01 (1.00)	0.001 ± 0.00 (1.00)	0.08 ± 0.02 (1.00)	0.29 ± 0.06 (1.00)
7396		41L/67N/69N/70R/215F	0.09 ± 0.01 (1.34)	0.001 ± 0.00 (1.00)	0.35 ± 0.07 (4.38)	3.83 ± 1.21 (13.21)
7406	190C	41L/69S*/74 V/184 V/210W/215Y	0.35 ± 0.04 (5.41)	1.09 ± 0.24 (1,090.00)	> 50 (> 625)	15.13 ± 2.16 (52.17)
7407	103N	70R/115F	19.69 ± 1.6 (328.16)	0.35 ± 0.03 (350.00)	> 50 (> 625)	> 50 (> 172)
12,227	101P/103N	41L/215Y	> 50 (> 833)	1.94 ± 0.23 (1,940.00)	> 50 (> 625)	1.00 ± 0.13 (3.48)
12,231	103N/179F/181C	41L/215F	> 50 (> 833)	0.18 ± 0.22 (180.00)	> 50 (> 625)	0.63 ± 0.19 (2.17)
12,241	101E/138G/190S		4.57 ± 2.3 (71. 41)	2.16 ± 0.51 (2,160.00)	> 50 (> 625)	0.08 ± 0.03 (0.28)
12,243	100I/179D/230L	41L/67G/74I	> 50 (> 833)	10.82 ± 0.37 (10,820.00)	21.45 ± 2.21 (268.13)	0.29 ± 0.01 (1.00)

[a] Catalog number provided by the NIH HIV Reagent Program

[b] The half maximal effective concentration

[c] The fold-change (FC) values were calculated by dividing the drug-resistant mutant HIV-1 EC_{50} by the wild type EC_{50}

[*] Indicates the insertion mutation

Table 3 The antiviral effect of BPPT on NNRTI-resistance associated single mutations

Virus	**EC_{50} (μM)[a] (Fold Change, FC)[b]**			
	BPPT	**EFV**	**NVP**	**AZT**
WT	0.06 ± 0.01 (1.00)	0.001 ± 0.00 (1.00)	0.08 ± 0.02 (1.00)	0.29 ± 0.06 (1.00)
L100I	3.50 ± 0.65 (58.33)	0.02 ± 0.00 (20.00)	0.18 ± 0.04 (2.25)	0.07 ± 0.01 (0.24)
K101P	1.71 ± 0.03 (28.50)	0.02 ± 0.00 (20.00)	8.31 ± 0.60 (103.88)	0.04 ± 0.00 (0.14)
K103N	0.88 ± 0.12 (14.67)	0.04 ± 0.01 (40.00)	4.55 ± 0.27 (56.88)	0.11 ± 0.01 (0.38)
V106M	0.07 ± 0.01 (1.10)	0.01 ± 0.00 (10.00)	1.71 ± 0.04 (21.37)	0.08 ± 0.01 (0.27)
Y181C	> 50 (> 833)	0.04 ± 0.00 (40.00)	19.49 ± 0.19 (203.63)	0.76 ± 0.03 (2.62)
Y181V	> 50 (> 833)	0.10 ± 0.00 (100.00)	> 50 (> 625)	4.11 ± 0.01 (14.17)
Y188L	> 50 (> 833)	0.26 ± 0.03 (260.00)	> 50 (> 625)	0.12 ± 0.01 (0.41)
G190A	0.07 ± 0.00 (1.17)	0.01 ± 0.00 (10.00)	15.66 ± 2.73 (197.75)	0.11 ± 0.01 (0.38)
G190C	0.29 ± 0.03 (4.83)	0.39 ± 0.09 (390.00)	23.77 ± 3.31 (297.13)	0.05 ± 0.01 (0.17)
G190S	0.28 ± 0.05 (4.67)	0.12 ± 0.01 (120.00)	32.69 ± 4.49 (408.63)	0.08 ± 0.01 (0.28)

[a] The half maximal effective concentration

[b] The fold-change (FC) values were calculated by dividing the drug-resistant mutant HIV-1 EC_{50} by the wild type EC_{50}

resistance-associated mutations except for Y181V. These data indicate that the mechanism underlying the inhibition of RTase by BPPT may be largely shared with those of NVP and EFV, with minor differences. These results also suggest that BPPT could be an effective therapeutic candidate against NNRTI-resistant viruses with a G190 mutation.

Combinatorial effect of BPPT with other classes of anti-HIV drugs

As uncompetitive binding to the targets of different classes of drugs can confer a higher barrier to drug resistance and an efficient therapeutic outcome, cARTs are medicated with combinations that generally consist of two NRTIs and either an NNRTI, INsTI, or a PRI [20, 52]. Accordingly, a drug combination assay was performed using TZM-bl cells treated with BPPT in combination with RTIs or INIs at their EC_{50}. Each combination showed an additive inhibitory effect on viral infectivity (Fig. 3A and B). The inhibitory effect of BPPT combined with EFV was slightly lower than that of combinations with other drugs, such as AZT, RAL, or DTG. The combinatorial inhibitory effects of PRIs were determined using multi-round viral replication in A3.01 cells infected with HIV-1 because PRIs act on the virus maturation step, followed by inhibition of viral infection of neighboring cells. As shown in Fig. 3D, the combination of BPPT and PRIs (LPV or RTV) significantly decreased the viral replication (Fig. 3D). However, these combinations were not cytotoxic (Fig. 3C and E). These results indicated that BPPT cooperatively inhibited the viral activity with other classes of ARVs and could be used as a component in cART.

Resistance selection of BPPT and molecular docking analysis of BPPT in HIV-1 RT

Susceptibility to BPPT was greatly reduced by substitutions at Y181 and Y188 in RTase and moderately reduced by substitutions at K101 and K103, whereas, BPPT was susceptible to substitutions at V106 and G190 (Table 3). Although these mutations are known to be clinically derived (N)NRTI resistance-associated mutations, BPPT-induced resistance mutations remain to be elucidated. Therefore, a resistance selection assay with a long-term BPPT treatment was conducted. A3.01 cells infected with HIV-1_{NL4-3} were initially treated with BPPT at its EC_{50}. The infected cells were passaged every 3–4 days with a twofold increase in concentration, and viral RNA was extracted from the viral supernatants on days 36, 39, and 52 for next-generation sequencing. Nine different variants, including L100I, K101E, V108I, E138G, V179I, Y181C/H, G190C, and H221Y, were detected in the culture with BPPT. Among them, the Y181C substitution was the most dominantly observed at a rate of 24.88% on day 36 (16-fold of EC_{50}), 36.5% on day 39 (17-fold of EC_{50}), and 72.1% on day 52 (18-fold of EC_{50}). The L100I substitution also emerged at a rate of 62.79% on day 36, but the proportion was gradually decreased to 41.82% and 26.6% on days 39 and 52, respectively. (Fig. 4A and Table S2). In addition, BPPT treatment caused the E138G and Y181H substitutions at rates of ~ 10% and G190C and H221Y at minor ratios (rates < 2%). EFV treatment produced 16 variants, including L100I, K101E, K103N, V106I, V108I, E138K/G, Y181C/H, G190C, H221Q/Y/N/K/stop, and p225H substitutions. Among these, the L100I substitution was the most dominant, and the proportion of the mutation was rapidly increased at a

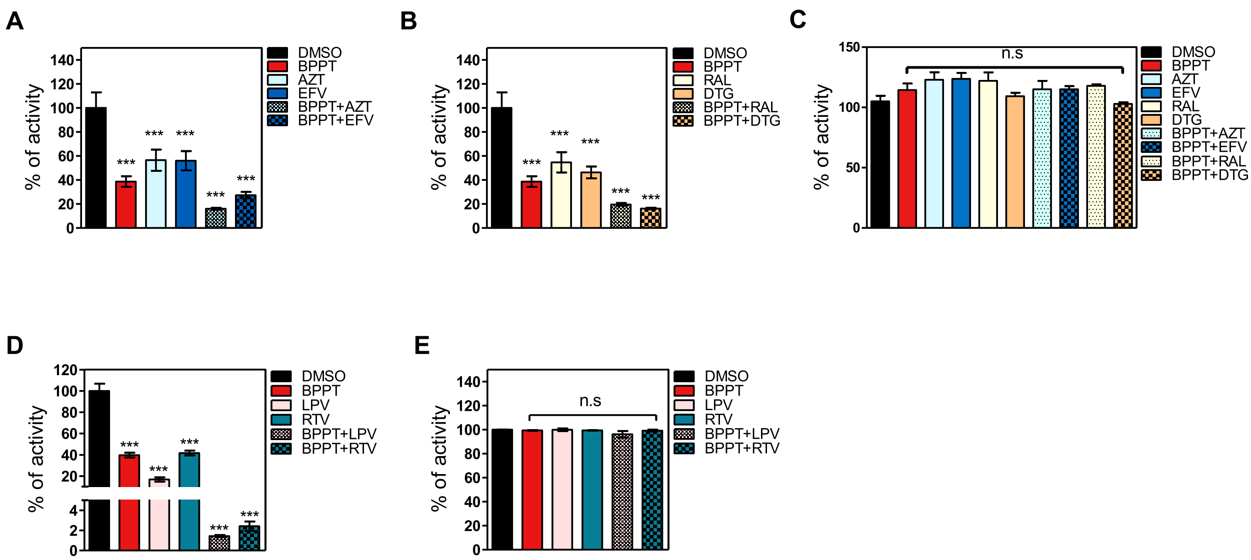

Fig. 3 Drug combination assay. **A**, **B** TZM-bl cells (1×10^4) infected with HIV-1_{NL4-3} at an MOI of 0.5 were treated with the indicated compounds at their EC_{50}. After 48 h of infection, the viral infectivity was determined using the Bright-Glo luciferase assay kit. The relative activity is expressed as the mean ± SD ($n = 3$) compared with the DMSO control. The EC_{50} values of the compounds are follows: BPPT (60 nM); AZT (290 nM); EFV (1 nM); RAL (10.4 nM); DTG (1.6 nM). **C** The cell viability was determined using the PrestoBlue Cell Viability Reagent under conditions described for A and B without viral infection. **D** A3.01 cells (5×10^4) infected with HIV-1_{NL4-3}IRES-eGFP at an MOI of 0.2 were treated with the indicated compounds at their EC_{50}. After 4 days of infection, the level of viral replication was determined by counting the GFP-positive cells using flow cytometry. The EC_{50} values of compounds are follows: lopinavir (LPV, 50 nM); ritonavir (RTV, 200 nM). The relative activity is expressed as the mean ± SD ($n = 3$) compared with the DMSO control. **E** The cell viability was determined under conditions described for **D**, without virus infection, using the PrestoBlue Cell Viability Reagent. **A**–**E** ***$p < 0.0001$, compared with the DMSO control. n.s.: non-significant

rate of 22.22%, 86.2%, and 97.63% on days 36, 39, and 52, respectively. The V108I, Y181C, and G190C mutations were detected at moderate rates (< 10%), whereas K101E and H221Q were present in minor proportions in EFV-treated viruses. RPV induced 15 different variants, including L100I, K101E, K106A, V108I, E138K, Y188stop, G190E/K/C/D/R, and H221Q/N/K/L/I. In the case of RPV, the E138K substitution was dominant, with mutation rate reaching 99.2% on day 52 (sixfold of EC_{50}). In addition, RPV induced the G190E substitution at a rate 20% and H221Q at a rate 10% on day 52. No amino acid substitution was found within the RT on day 52 in the no-drug control group (Fig. 4A). These data indicate that the escape pressure of the virus conferred by BPPT may be different from that of EFV or RPV, especially the L100 and Y188 residues, which play important roles in the antiviral activity of BPPT.

To determine the mode of molecular binding of BPPT to the NNRTI-binding pocket (NNIBP) in RTase, in silico molecular docking analysis of BPPT was performed using the X-ray crystal structure of HIV-1 RTase (PDB ID:1IKW) and EFV as a reference standard [50]. The docking results showed that BPPT and EFV occupied the same hydrophobic NNIBP, and the overall binding shape was similar, whereas the details of the binding mode of BPPT were somewhat different from those of EFV (Fig. 4B). The most distinctive feature was the number of hydrogen bonds (H-bonds). H-bonding is one of the most important interactions in biomolecular systems. In general, because the interaction strength of H-bond is relatively high, the number of H-bonds can be a good reference for comparing the binding affinity of ligands with proteins. Based on molecular docking results, it was predicted that BPPT forms three H-bonds with the K101 residue of the protein, whereas EFV forms only one. Thus, BPPT might be assumed to bind more tightly or strongly to the protein than does EFV. This result is consistent with our experimental data. The 2D interaction analysis provided more details on the interaction (Fig. 4C). Three H-bonds of BPPT are generated via an NH moiety and two nitrogen atoms (2, 3-N) in the thiadiazole core with K101, whereas one H-bond in EFV is created between the NH group in benzoxazinone and the protein. A phenyl moiety appended to the pyrazole of BPPT participated in the pi-pi stacked interaction with the phenyl group in Y181 and the indole moieties in W229. Additional interactions, including van der Waals, hydrophobic, pi-alkyl, and alkyl interactions, were also visualized.

Another remarkable result was found for the G190 residue of RTase. The antiviral effect data showed that BPPT had significantly better drug resistance than EFV with the

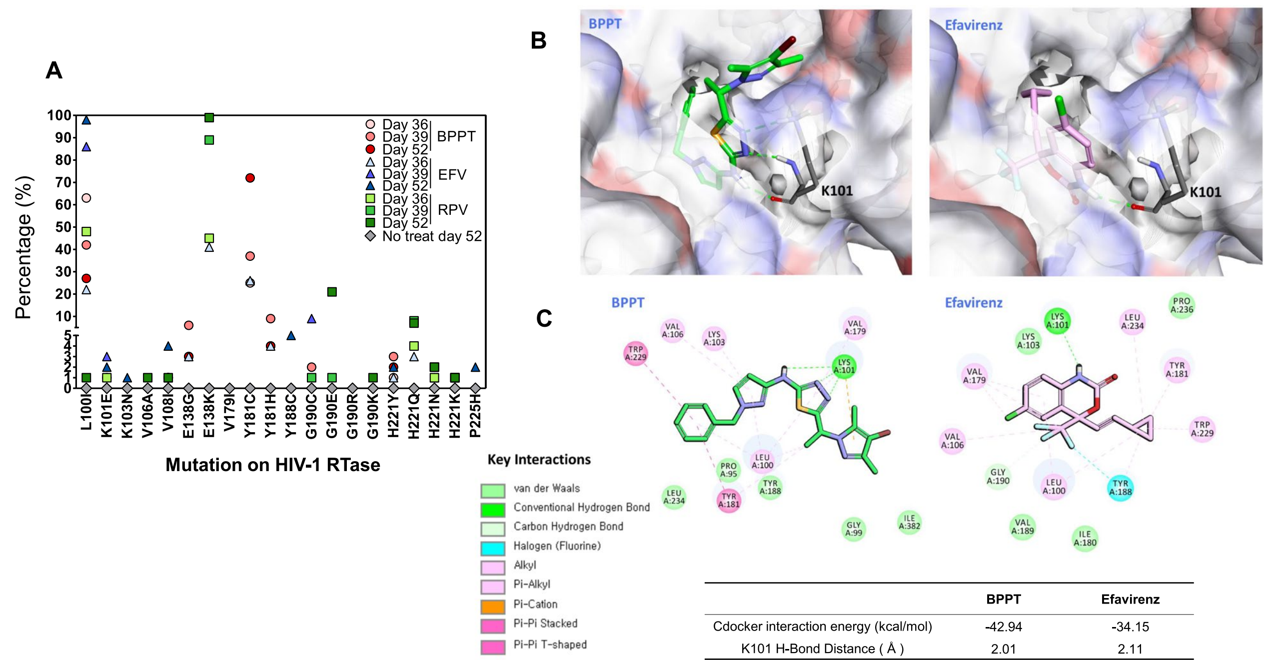

	BPPT	Efavirenz
Cdocker interaction energy (kcal/mol)	-42.94	-34.15
K101 H-Bond Distance (Å)	2.01	2.11

Fig. 4 In vitro selection of drug resistance mutations and molecular docking study. **A** Selection of drug resistance mutations. A3.01 cells (1×10^5) infected with HIV-1_{NL4-3} at an MOI of 0.5 were treated with the following compounds at their EC_{50} values: BPPT (60 nM), EFV (1 nM), and RPV (0.7 nM). Every 3–4 days, the infected cells and supernatant were passaged. At 36, 39, and 52 days after infection, the viral RNA was extracted from the viral supernatant and the mutations were analyzed using next-generation sequencing as described in "Materials and Methods." The dots indicate the percent of the mutation in the total read. **B** 3D binding modes of BPPT and EFV with HIV-1 RTase. The green lines represent the hydrogen bonds, which are among the most important and strong interactions between protein and ligands. **C** 2D interaction maps of BPPT and EFV with HIV-1 RTase. The interaction networks between the atoms in the ligands with the protein were analyzed using the 2-dimensional map. Different colors of dotted lines represent different molecular interactions as shown in the legend. Data for the Cdocker interaction energy and H-bond distance from the K101 residue are given at the bottom

G190 mutants (Table 3). The experimental results corroborated our computer modeling study because the 2D binding network map clearly showed that EFV interacted with G190, but BPPT did not (Fig. 4C). The CDocker interaction energy of BPPT was − 42.94 kcal/mol, which was lower than that of EFV (− 34.15 kcal/mol). These data indicate that BPPT may bind to NNIBP as previously reported for NNRTIs, with some minor differences in the interaction pattern from these drugs. Overall, our in silico analysis indicated that BPPT shows better affinity than EFV for the protein based on the number of H-bonds and docking scores and has a more favorable binding mode for drug resistance.

Discussion

Thiadiazoles are heterocyclic compounds containing two nitrogens, which have been extensively studied owing to their pharmacological and biological properties, such as antibacterial, antifungal, antitubercular, and antiviral effects. In particular, several compounds containing thiadiazoles, including 4-phenyl-l,2,5-thiadiazol-3-yl N,N-dialkylcarbamate (TDA) [53], 1,2,3-thiadiazole thioacetanilides (TTA) [54], and 3-aryl-6-adamantylmethyl-[1,2,4]triazolo[3,4-b][1,3,4]thiadiazoles [55], were suggested as good scaffolds for the anti-HIV-1 activity. Pyrazoles are also an important class of heterocyclic nuclei in medicinal chemistry because of their varied biological activities, including antiviral, antimicrobial, anticancer, and anti-inflammatory effects. Some pyrazole derivatives have been reported to have anti-HIV-1 activity [56–59] and were reported to act through RTase inhibition. Despite the potency of thiadiazole and pyrazole structures in the inhibition of HIV-1, the thiadiazole–pyrazole hybrid has not been explored in the development of anti-HIV-1 agents.

In this study, a thiadiazole derivative (BPPT) harboring two pyrazoles was identified as an inhibitor of HIV-1 infection using a cell-based screening of a compound library. BPPT exhibited high potency with an EC_{50} of 60 nM and had no cytotoxicity up to 250 μM, resulting in an SI value > 4166.7, which might be comparable to that of the approved ARVs (Table 1). BPPT showed a TOA curve similar to that of EFV (Fig. 2A), clear inhibitory effects on both in vitro and in vivo RTase activities

(Fig. 2D and E), and a well-fitted docking mode with the NNIBP of RTase (Fig. 4B and C). These data demonstrate that BPPT is a novel NNRTI.

The current clinical use of NNRTI drugs has limited therapeutic value because of the emergence of multi-drug-resistant variants. First-generation NNRTIs (NVP, DLV, and EFV) have lower genetic barriers to resistance than other ARVs [60, 61]. The most common NNRTI resistance-associated mutations, such as K103N, Y181C, and G190A, were detected in patients in whom first-line therapy failed [60, 61]. Second-generation NNRTIs (etravirine [ETR] and RPV) belong to the family of di-arylpyrimidine (DAPY) compounds that display potent antiviral activities against wild-type HIV-1 and first-generation NNRTI resistance-associated mutations, especially K103N and Y181C mutations [62]. Nevertheless, Y181I, Y181V, E138K, and K103N/Y181C mutations significantly decrease the susceptibility to second-generation NNRTIs [60, 61, 63]. Furthermore, these drugs have poor water solubility and pharmacokinetic properties [64]. Recently, doravirine (DOR), with a relatively high genetic barrier to resistance-associated mutations and potent antiviral activity, was approved [65, 66]; however, high levels of resistance-associated mutations, such as V106M/A, Y188L, and M230L, restrict its clinical use [66].

BPPT has a unique structural feature that may provide resistance mutation profiles different from those of previous NNRTIs. BPPT (FC = 28.5) exhibited decreased susceptibility of the K101P mutant compared to EFV (FC = 17) (Table 3), indicating that the NH group and thiadiazole moiety of BPPT are crucial for interaction with K101 through three hydrogen bonds (Fig. 4C). Mutations at Y181 and Y188 completely abrogated the antiviral activity of BPPT, indicating that the hydrophobic tunnel provided by these amino acids may allow suitable interactions between BPPT and NNIBP. In particular, the aromatic stacking interaction with Y181 in the phenyl moiety of BPPT is similar to that of the chlorophenol moiety in RPV and DOL [67]. Mutations at G190 (such as G190A and 190S), observed frequently in patients who received first-generation NNRTIs [60, 61], showed high levels of resistance to EFV and NVP; however, these mutations were inadequate for conferring severe resistance to BPPT (Table 3). These data are concordant with the docking simulation results showing no interaction between BPPT and G190 (Fig. 4C). This phenomenon is similar to the potency of DOR against G190A, but modest resistance against G190S [67, 68]. In vitro selection of resistance mutations for BPPT showed patterns different from those for EFV and RPV. EFV exhibited well-characterized resistance-associated mutations, including L1001, Y188C, G190C, and RPV, as well as E138K, G190E, and H221Q [44, 68, 69]. Upon treatment with BPPT, Y181C, Y181H, and L100I were generally observed, whereas V106A, V108I, L234I, and F227L, which are known to be selected by DOR [66, 68], were not detected. These data indicate that the L101 and Y181 residues are critical for interaction with BPPT, as shown in the docking model (Fig. 4C), whereas the hydrophobic residues V106 and V108, known to interact with DOR [44, 67] are not important for the BPPT activity to the extent they are for DOR. The differences in the potency of resistance-associated mutations and in vitro resistance selection profiles might be due to the unique structure of BPPT, apart from the structures of previously developed NNRTIs.

Second-generation NNRTIs, such as DAPY (ETR, RPV) or its modified form (DOR), are multi-ring types, which may provide flexibility to improve the ability to bind to NNIBP and overcome resistance-associated mutations [44, 70]. In this context, BPPT also comprises multifunctional ring moieties, which may provide the flexibility to interact with NNIBP and/or avoid NNRTI-resistant mutations, unlike the DAPY-shaped drugs.

The (pyrazol-3-YL)-1,3,4-thiadiazol-2-amine and (pyrazol-3-YL)-1,3,4-thiazol-2-amine compounds, which are similar in structure to BPPT, were identified as inhibitors of the enoyl acyl carrier protein reductase (InhA) enzyme of *Mycobacterium tuberculosis* (Mtb) [71]. Interestingly, the Mtb-inhibitory compounds have a core structure of 2-amino-(pyrazole-3-yl)-thiadiazole, which is same as that of BPPT with some differences from the BPPT at several residues (Fig. S8). The additive effects of BPPT observed in combination with other ARVs indicated that BPPT may be potentially useful for treating infected patients in combination with the currently used anti-HIV-1 drugs.

Although the core structure of BPPT is not originative and its potency is lesser than that of the current ARVs, the limitation of BPPT could be overcome if its potency is further improved by undertaking a structure–activity relationship study in conjunction with determination of the actual binding to NNIBP and in vivo characterization.

Conclusion

We identified BPPT, which inhibits HIV-1 infectivity and replication cycle in various cells, as well as HIV-1 variants, and exhibits low cytotoxicity. Mechanistic analyses revealed that BPPT is an inhibitor of the HIV-1 RTase activity with a mode of action similar to that of NNRTIs. A series of studies on the susceptibility of NNRTI resistance-associated mutants, molecular docking to RTase, and in vitro resistance selection demonstrated that BPPT might occupy the NNIBP of RTase differently from the currently used NNRTIs. Taken together, BPPT, comprising four aromatic rings, could serve as a promising scaffold for the development of a new NNRTI against the current NNRTI-resistant HIV-1 variants.

Supplementary Information

The online version contains supplementary material available at https://doi.org/10.1186/s12985-025-02680-3.

Supplementary file 1.

Supplementary file 2.

Acknowledgements
The chemical library used in this study was kindly provided by the Korea Chemical Bank (www.chembank.org) of the Korea Research Institute of Chemical Technology. We appreciate Yeon-Jung Kim in the Division of Biomedical Research Institution, National Institute of Health, for assistance with next-generation sequencing analysis.

Author contributions
Conceptualization, C.Y.; methodology, K.Y., Y.S., D.K., J.K., J.K., P.S., and K.W.L; validation, K.Y., Y.S., and D.K.; formal analysis, K.Y., Y.S., D.K., J.K., J.K., K.W.L., and C.M.P.; investigation, K.Y., Y.S., D.K., J.K., J.K., P.S., and K.W.L.; Resources, H.K. and S.K.; data curation, K.Y. and J.K.; writing—original draft preparation, K.Y. and C.Y.; writing—review and editing, C.Y.; visualization, K.Y., P.S., and K.W.L.; supervision, C.Y. and S.B.; project administration, C.Y. and S.B.; funding acquisition, S.B. All authors have read and agreed to the published version of the manuscript.

Funding
This study was supported by the Korea National Institute of Health (KNIH) (No. 2022-NI-006).

Availability of data and materials
The data supporting the findings of this study are available upon request from the corresponding author.

Declarations

Ethics approval and consent to participate
Not applicable.

Consent for publication
Not applicable.

Competing interests
The authors declare no competing interests.

Author details
[1]Division of Chronic Viral Diseases, Center for Emerging Virus Research, Korea National Institute of Health, 187 Osongsaengmyeong 2-ro, Cheongju 28159, Republic of Korea. [2]Division of Emerging Infectious Diseases, Department of Laboratory Diagnosis and Analysis, Korea Disease Control and Prevention Agency, 187 Osongsaengmyeong 2-ro, Cheongju 28159, Republic of Korea. [3]Division of Applied Life Science (BK21 Four), Plant Molecular Biology and Biotechnology Research Center (PMBBRC), Gyeongsang National University (GNU), 501 Jinju-daero, Jinju 52828, Republic of Korea. [4]Angel i-Drug Design (AiDD), 33-3 Jinyangho-ro 44, Jinju 52650, Republic of Korea. [5]Quantum-AI Lab, Korea Quantum Computing (KQC), 55 Centumjungang-ro, Busan 48058, Republic of Korea. [6]Infectious Diseases Therapeutic Research Center, Korea Research Institute of Chemical Technology, Daejeon 34114, Republic of Korea. [7]Drug Information Research Center, Korea Research Institute of Chemical Technology, Daejeon 34114, Republic of Korea.

Received: 15 October 2024 Accepted: 23 February 2025
Published online: 07 March 2025

References

1. Global HIV & AIDS Statistics https://www.unaids.org/en/resources/fact-sheet (updated 2 August 2024) [https://www.unaids.org/en/resources/fact-sheet]
2. Deeks SG, Grant RM, Wrin T, Paxinos EE, Liegler T, Hoh R, Martin JN, Petropoulos CJ. Persistence of drug-resistant HIV-1 after a structured treatment interruption and its impact on treatment response. AIDS. 2003;17(3):361–70.
3. Finzi D, Hermankova M, Pierson T, Carruth LM, Buck C, Chaisson RE, Quinn TC, Chadwick K, Margolick J, Brookmeyer R, et al. Identification of a reservoir for HIV-1 in patients on highly active antiretroviral therapy. Science. 1997;278(5341):1295–300.
4. Wong JK, Hezareh M, Gunthard HF, Havlir DV, Ignacio CC, Spina CA, Richman DD. Recovery of replication-competent HIV despite prolonged suppression of plasma viremia. Science. 1997;278(5341):1291–5.
5. Chun TW, Stuyver L, Mizell SB, Ehler LA, Mican JA, Baseler M, Lloyd AL, Nowak MA, Fauci AS. Presence of an inducible HIV-1 latent reservoir during highly active antiretroviral therapy. Proc Natl Acad Sci USA. 1997;94(24):13193–7.
6. Galli L, Parisi MR, Poli A, Menozzi M, Fiscon M, Garlassi E, Francisci D, Di Biagio A, Sterrantino G, Fornabaio C, et al. Burden of disease in pwh harboring a multidrug-resistant virus: data from the PRESTIGIO registry. Open Forum Infect Dis. 2020;7(11):offa456.
7. Baba M, Nishimura O, Kanzaki N, Okamoto M, Sawada H, Iizawa Y, Shiraishi M, Aramaki Y, Okonogi K, Ogawa Y, et al. A small-molecule, nonpeptide CCR5 antagonist with highly potent and selective anti-HIV-1 activity. Proc Natl Acad Sci USA. 1999;96(10):5698–703.
8. Dorr P, Westby M, Dobbs S, Griffin P, Irvine B, Macartney M, Mori J, Rickett G, Smith-Burchnell C, Napier C, et al. Maraviroc (UK-427,857), a potent, orally bioavailable, and selective small-molecule inhibitor of chemokine receptor CCR5 with broad-spectrum anti-human immunodeficiency virus type 1 activity. Antimicrob Agents Chemother. 2005;49(11):4721–32.
9. Derdeyn CA, Decker JM, Sfakianos JN, Zhang Z, O'Brien WA, Ratner L, Shaw GM, Hunter E. Sensitivity of human immunodeficiency virus type 1 to fusion inhibitors targeted to the gp41 first heptad repeat involves distinct regions of gp41 and is consistently modulated by gp120 interactions with the coreceptor. J Virol. 2001;75(18):8605–14.
10. Furman PA, Fyfe JA, St Clair MH, Weinhold K, Rideout JL, Freeman GA, Lehrman SN, Bolognesi DP, Broder S, Mitsuya H, et al. Phosphorylation of 3′-azido-3′-deoxythymidine and selective interaction of the 5′-triphosphate with human immunodeficiency virus reverse transcriptase. Proc Natl Acad Sci USA. 1986;83(21):8333–7.
11. Merluzzi VJ, Hargrave KD, Labadia M, Grozinger K, Skoog M, Wu JC, Shih CK, Eckner K, Hattox S, Adams J, et al. Inhibition of HIV-1 replication by a nonnucleoside reverse transcriptase inhibitor. Science. 1990;250(4986):1411–3.
12. Markowitz M, Morales-Ramirez JO, Nguyen BY, Kovacs CM, Steigbigel RT, Cooper DA, Liporace R, Schwartz R, Isaacs R, Gilde LR, et al. Antiretroviral activity, pharmacokinetics, and tolerability of MK-0518, a novel inhibitor of HIV-1 integrase, dosed as monotherapy for 10 days in treatment-naive HIV-1-infected individuals. J Acquir Immune Defic Syndr. 2006;43(5):509–15.
13. Roberts NA, Martin JA, Kinchington D, Broadhurst AV, Craig JC, Duncan IB, Galpin SA, Handa BK, Kay J, Krohn A, et al. Rational design of peptide-based HIV proteinase inhibitors. Science. 1990;248(4953):358–61.
14. Li G, Wang Y, De Clercq E. Approved HIV reverse transcriptase inhibitors in the past decade. Acta Pharm Sin B. 2022;12(4):1567–90.
15. Anderson PL, Kakuda TN, Lichtenstein KA. The cellular pharmacology of nucleoside- and nucleotide-analogue reverse-transcriptase inhibitors and its relationship to clinical toxicities. Clin Infect Dis Off Publ Infect Dis Soc Am. 2004;38(5):743–53.
16. Tuske S, Sarafianos SG, Clark AD Jr, Ding J, Naeger LK, White KL, Miller MD, Gibbs CS, Boyer PL, Clark P, et al. Structures of HIV-1 RT-DNA complexes before and after incorporation of the anti-AIDS drug tenofovir. Nat Struct Mol Biol. 2004;11(5):469–74.
17. Ren J, Esnouf R, Garman E, Somers D, Ross C, Kirby I, Keeling J, Darby G, Jones Y, Stuart D, et al. High resolution structures of HIV-1 RT from four RT-inhibitor complexes. Nat Struct Biol. 1995;2(4):293–302.
18. Kohlstaedt LA, Wang J, Friedman JM, Rice PA, Steitz TA. Crystal structure at 3.5 A resolution of HIV-1 reverse transcriptase complexed with an inhibitor. Science. 1992;256(5065):1783–90.

19. Esnouf R, Ren J, Ross C, Jones Y, Stammers D, Stuart D. Mechanism of inhibition of HIV-1 reverse transcriptase by non-nucleoside inhibitors. Nat Struct Biol. 1995;2(4):303–8.
20. Vanangamudi M, Palaniappan S, Kathiravan MK, Namasivayam V. Strategies in the design and development of non-nucleoside reverse transcriptase inhibitors (NNRTIs). Viruses. 2023;15(10):1992.
21. Vanangamudi M, Kurup S, Namasivayam V. Non-nucleoside reverse transcriptase inhibitors (NNRTIs): a brief overview of clinically approved drugs and combination regimens. Curr Opin Pharmacol. 2020;54:179–87.
22. Ordonez P, Hamasaki T, Isono Y, Sakakibara N, Ikejiri M, Maruyama T, Baba M. Anti-human immunodeficiency virus type 1 activity of novel 6-substituted 1-benzyl-3-(3,5-dimethylbenzyl)uracil derivatives. Antimicrob Agents Chemother. 2012;56(5):2581–9.
23. Mellors J, Larder B, Schinazi R. Mutations in HIV-1 reverse transcriptase and protease associated with drug resistance. J Acquir Immune Defic Syndr. 1995;10:S45–S45.
24. Alcaro S, Alteri C, Artese A, Ceccherini-Silberstein F, Costa G, Ortuso F, Bertoli A, Forbici F, Santoro MM, Parrotta L, et al. Docking analysis and resistance evaluation of clinically relevant mutations associated with the HIV-1 non-nucleoside reverse transcriptase inhibitors nevirapine, efavirenz and etravirine. ChemMedChem. 2011;6(12):2203–13.
25. Platt EJ, Bilska M, Kozak SL, Kabat D, Montefiori DC. Evidence that ecotropic murine leukemia virus contamination in TZM-bl cells does not affect the outcome of neutralizing antibody assays with human immunodeficiency virus type 1. J Virol. 2009;83(16):8289–92.
26. Xing L, Wang S, Hu Q, Li J, Zeng Y. Comparison of three quantification methods for the TZM-bl pseudovirus assay for screening of anti-HIV-1 agents. J Virol Methods. 2016;233:56–61.
27. Wei X, Decker JM, Liu H, Zhang Z, Arani RB, Kilby JM, Saag MS, Wu X, Shaw GM, Kappes JC. Emergence of resistant human immunodeficiency virus type 1 in patients receiving fusion inhibitor (T-20) monotherapy. Antimicrob Agents Chemother. 2002;46(6):1896–905.
28. Vicenzi E, Poli G. Infection of CD4+ primary T cells and cell lines, generation of chronically infected cell lines, and induction of HIV expression. Curr Protoc Immunol. 2005;69:12.
29. Balamane M, Varghese V, Melikian GL, Fessel WJ, Katzenstein DA, Shafer RW. Panel of prototypical recombinant infectious molecular clones resistant to nevirapine, efavirenz, etravirine, and rilpivirine. Antimicrob Agents Chemother. 2012;56(8):4522–4.
30. Johnston E, Dupnik KM, Gonzales MJ, Winters MA, Rhee SY, Imamichi T, Shafer RW. Panel of prototypical infectious molecular HIV-1 clones containing multiple nucleoside reverse transcriptase inhibitor resistance mutations. AIDS. 2005;19(7):731–3.
31. Schindler M, Wurfl S, Benaroch P, Greenough TC, Daniels R, Easterbrook P, Brenner M, Munch J, Kirchhoff F. Down-modulation of mature major histocompatibility complex class II and up-regulation of invariant chain cell surface expression are well-conserved functions of human and simian immunodeficiency virus nef alleles. J Virol. 2003;77(19):10548–56.
32. Shin Y, Kim HG, Park CM, Choi MS, Kim DE, Choi BS, Kim K, Yoon CH. Identification of novel compounds against Tat-mediated human immunodeficiency virus-1 transcription by high-throughput functional screening assay. Biochem Biophys Res Commun. 2020;523(2):368–74.
33. Kimpton J, Emerman M. Detection of replication-competent and pseudotyped human immunodeficiency virus with a sensitive cell line on the basis of activation of an integrated beta-galactosidase gene. J Virol. 1992;66(4):2232–9.
34. Horton RM, Hunt HD, Ho SN, Pullen JK, Pease LR. Engineering hybrid genes without the use of restriction enzymes: gene splicing by overlap extension. Gene. 1989;77(1):61–8.
35. Daelemans D, Pauwels R, De Clercq E, Pannecouque C. A time-of-drug addition approach to target identification of antiviral compounds. Nat Protoc. 2011;6(6):925–33.
36. Kim MJ, Kim SH, Park JA, Yu KL, Jang SI, Kim BS, Lee ES, You JC. Identification and characterization of a new type of inhibitor against the human immunodeficiency virus type-1 nucleocapsid protein. Retrovirology. 2015;12:90.
37. Marino-Merlo F, Frezza C, Papaianni E, Valletta E, Mastino A, Macchi B. Development and evaluation of a simple and effective RT-qPCR inhibitory assay for detection of the efficacy of compounds towards HIV reverse transcriptase. Appl Microbiol Biotechnol. 2017;101(22):8249–58.
38. Laura G, Moran SP, Ro S, de Noronha CM, Shi B. Analysis of early phase HIV-1 replication and integration events by using real-time PCR. Bio-Protoc. 2019;9(4):e3168–e3168.
39. Kim MJ, Yu KL, Han R, Lee Y, Oh K, You JC. Identification of a non-nucleoside reverse transcriptase inhibitor against human immunodeficiency virus-1. ACS Infect Dis. 2023;9(8):1582–92.
40. Vandergeeten C, Fromentin R, Merlini E, Lawani MB, DaFonseca S, Bakeman W, McNulty A, Ramgopal M, Michael N, Kim JH, et al. Cross-clade ultrasensitive PCR-based assays to measure HIV persistence in large-cohort studies. J Virol. 2014;88(21):12385–96.
41. Park KH, Kim M, Bae SE, Lee HJ, Kim KC, Choi BS, Kim YB. Study on suitable analysis method for HIV-1 non-catalytic integrase inhibitor. Virol J. 2021;18(1):17.
42. Lisovsky I, Schader SM, Martinez-Cajas JL, Oliveira M, Moisi D, Wainberg MA. HIV-1 protease codon 36 polymorphisms and differential development of resistance to nelfinavir, lopinavir, and atazanavir in different HIV-1 subtypes. Antimicrob Agents Chemother. 2010;54(7):2878–85.
43. Koh Y, Das D, Leschenko S, Nakata H, Ogata-Aoki H, Amano M, Nakayama M, Ghosh AK, Mitsuya H. GRL-02031, a novel nonpeptidic protease inhibitor (PI) containing a stereochemically defined fused cyclopentanyltetrahydrofuran potent against multi-PI-resistant human immunodeficiency virus type 1 in vitro. Antimicrob Agents Chemother. 2009;53(3):997–1006.
44. Cilento ME, Kirby KA, Sarafianos SG. Avoiding drug resistance in HIV reverse transcriptase. Chem Rev. 2021;121(6):3271–96.
45. Meng XY, Zhang HX, Mezei M, Cui M. Molecular docking: a powerful approach for structure-based drug discovery. Curr Comput Aided Drug Des. 2011;7(2):146–57.
46. Singh P, Kumar V, Lee KW, Hong JC. Discovery of novel allosteric SHP2 inhibitor using pharmacophore-based virtual screening, molecular docking, molecular dynamics simulation, and principal component analysis. Pharmaceuticals. 2024;17(7):935.
47. Dassault systemes BIOVIA, Discovery studio modelling environment, Release 4.5. Accelrys Software Inc. [https://www.3ds.com/products/biovia/discovery-studio]
48. Yadav MB, Singh P, Jeong YT. Regioselective synthesis and molecular docking studies of functionalized imidazo [1,2-a]pyridine derivatives through MCRs. Mol Divers. 2024;28(1):171–82.
49. Singh P, Kumar V, Lee G, Jung TS, Ha MW, Hong JC, Lee KW. Pharmacophore-oriented identification of potential leads as CCR5 inhibitors to block HIV cellular entry. Int J Mol Sci. 2022;23(24):16122.
50. Lindberg J, Sigurdsson S, Lowgren S, Andersson HO, Sahlberg C, Noreen R, Fridborg K, Zhang H, Unge T. Structural basis for the inhibitory efficacy of efavirenz (DMP-266), MSC194 and PNU142721 towards the HIV-1 RT K103N mutant. Eur J Biochem. 2002;269(6):1670–7.
51. Sapay N, Tieleman DP. Combination of the CHARMM27 force field with united-atom lipid force fields. J Comput Chem. 2011;32(7):1400–10.
52. Kumar PN, Patel P. Lamivudine for the treatment of HIV. Expert Opin Drug Metab Toxicol. 2010;6(1):105–14.
53. Ijichi K, Fujiwara M, Nagano H, Matsumoto Y, Hanasaki Y, Ide T, Katsuura K, Takayama H, Shirakawa S, Aimi N, et al. Anti-HIV-1 activity of thiadiazole derivatives: structure-activity relationship, reverse transcriptase inhibition, and lipophilicity. Antivir Res. 1996;31(1–2):87–94.
54. Zhan P, Liu X, Li Z, Fang Z, Li Z, Wang D, Pannecouque C, Clercq ED. Novel 1,2,3-thiadiazole derivatives as HIV-1 NNRTIs with improved potency: synthesis and preliminary SAR studies. Bioorg Med Chem. 2009;17(16):5920–7.
55. Khan MUH, Hameed S, Farman M, Al-Masoudi NA, Stoeckli-Evans H. Synthesis, anti-HIV activity and molecular modeling study of 3-aryl-6-adamantylmethyl-[1, 2, 4] triazolo [3, 4-b][1, 3, 4] thiadiazole derivatives. Zeitschrift für Naturforschung B. 2015;70(8):609–16.
56. Tucker TJ, Sisko JT, Tynebor RM, Williams TM, Felock PJ, Flynn JA, Lai MT, Liang Y, McGaughey G, Liu M, et al. Discovery of 3-5-[(6-amino-1H-pyrazolo[3,4-b]pyridine-3-yl)methoxy]-2-chlorophenoxy-5-chlorobenzonitrile (MK-4965): a potent, orally bioavailable HIV-1 non-nucleoside reverse transcriptase inhibitor with improved potency against key mutant viruses. J Med Chem. 2008;51(20):6503–11.
57. Kumar S, Gupta S, Abadi LF, Gaikwad S, Desai D, Bhutani KK, Kulkarni S, Singh IP. Synthesis and in-vitro anti-HIV-1 evaluation of novel pyrazolo[4,3-c]pyridin-4-one derivatives. Eur J Med Chem. 2019;183:111714.

58. Mowbray CE, Burt C, Corbau R, Perros M, Tran I, Stupple PA, Webster R, Wood A. Pyrazole NNRTIs 1: design and initial optimisation of a novel template. Bioorg Med Chem Lett. 2009;19(19):5599–602.
59. Kim J, Lee D, Park C, So W, Jo M, Ok T, Kwon J, Kong S, Jo S, Kim Y, et al. Discovery of phenylaminopyridine derivatives as novel HIV-1 non-nucleoside reverse transcriptase inhibitors. ACS Med Chem Lett. 2012;3(8):678–82.
60. Melikian GL, Rhee SY, Varghese V, Porter D, White K, Taylor J, Towner W, Troia P, Burack J, Dejesus E, et al. Non-nucleoside reverse transcriptase inhibitor (NNRTI) cross-resistance: implications for preclinical evaluation of novel NNRTIs and clinical genotypic resistance testing. J Antimicrob Chemother. 2014;69(1):12–20.
61. Basson AE, Rhee SY, Parry CM, El-Khatib Z, Charalambous S, De Oliveira T, Pillay D, Hoffmann C, Katzenstein D, Shafer RW, et al. Impact of drug resistance-associated amino acid changes in HIV-1 subtype C on susceptibility to newer nonnucleoside reverse transcriptase inhibitors. Antimicrob Agents Chemother. 2015;59(2):960–71.
62. Huang B, Liu X, Tian Y, Kang D, Zhou Z, Daelemans D, De Clercq E, Pannecouque C, Zhan P, Liu X. First discovery of a potential carbonate prodrug of NNRTI drug candidate RDEA427 with submicromolar inhibitory activity against HIV-1 K103N/Y181C double mutant strain. Bioorg Med Chem Lett. 2018;28(8):1348–51.
63. Beyrer C, Pozniak A. HIV drug resistance-an emerging threat to epidemic control. N Engl J Med. 2017;377(17):1605–7.
64. Wang Y, De Clercq E, Li G. Current and emerging non-nucleoside reverse transcriptase inhibitors (NNRTIs) for HIV-1 treatment. Expert Opin Drug Metab Toxicol. 2019;15(10):813–29.
65. Saladini F, Giammarino F, Hosseini BA, Giannini A, Boccuto A, Dragoni F, Vicenti I, Shafer RW, Zazzi M. In vitro cross-resistance to doravirine in a panel of HIV-1 clones harbouring multiple NNRTI resistance mutations. J Antimicrob Chemother. 2021;76(1):130–4.
66. Brenner BG, Oliveira M, Ibanescu RI, Routy JP, Thomas R. Doravirine responses to HIV-1 viruses bearing mutations to NRTIs and NNRTIs under in vitro selective drug pressure. J Antimicrob Chemother. 2023;78(8):1921–8.
67. Smith SJ, Pauly GT, Akram A, Melody K, Ambrose Z, Schneider JP, Hughes SH. Rilpivirine and doravirine have complementary efficacies against NNRTI-resistant HIV-1 mutants. J Acquir Immune Defic Syndr. 2016;72(5):485–91.
68. Feng M, Wang D, Grobler JA, Hazuda DJ, Miller MD, Lai MT. In vitro resistance selection with doravirine (MK-1439), a novel nonnucleoside reverse transcriptase inhibitor with distinct mutation development pathways. Antimicrob Agents Chemother. 2015;59(1):590–8.
69. Kulkarni R, Babaoglu K, Lansdon EB, Rimsky L, Van Eygen V, Picchio G, Svarovskaia E, Miller MD, White KL. The HIV-1 reverse transcriptase M184I mutation enhances the E138K-associated resistance to rilpivirine and decreases viral fitness. J Acquir Immune Defic Syndr. 2012;59(1):47–54.
70. Prener L, Baszczynski O, Kaiser MM, Dracinsky M, Stepan G, Lee YJ, Brumshtein B, Yu H, Jansa P, Lansdon EB, et al. Design and synthesis of novel HIV-1 NNRTIs with bicyclic cores and with improved physicochemical properties. J Med Chem. 2023;66(3):1761–77.
71. Pages LBPJC, Menendez RF, Velando EPF, Del Valle SG, Diaz MLL, Losana AM, Wolfendale MJ. Glaxo Group: (pyrazol-3-yl) -1, 3, 4-thiadiazol-2-amine and (pyrazol-3-yl)-1, 3, 4-thiazol-2-amine compounds. In: US; 2010.
72. Lansdon EB, Brendza KM, Hung M, Wang R, Mukund S, Jin D, Birkus G, Kutty N, Liu X. Crystal structures of HIV-1 reverse transcriptase with etravirine (TMC125) and rilpivirine (TMC278): implications for drug design. J Med Chem. 2010;53(10):4295–9.

Publisher's Note